



This is the accepted manuscript made available via CHORUS. The article has been published as:

Spectroscopy of ${}^{13}\text{Be}$ through isobaric analog states in ${}^{13}\text{B}$

${}^{13}\text{Be}$ through isobaric analog states in ${}^{13}\text{B}$

${}^{13}\text{B}$

${}^{13}\text{B}$

C. Hunt, S. Ahn, J. Bishop, E. Koshchiy, E. Aboud, M. Alcorta, A. Bosh, K. Hahn, S. Han, C. E. Parker, E. C. Pollacco, B. T. Roeder, M. Roosa, S. Upadhyayula, A. S. Volya, and G. V. Rogachev

Phys. Rev. C **108**, L051606 — Published 20 November 2023

DOI: [10.1103/PhysRevC.108.L051606](https://doi.org/10.1103/PhysRevC.108.L051606)

Spectroscopy of ^{13}Be through isobaric analogue states in ^{13}B

C. Hunt,^{1,2,*} S. Ahn,^{2,†} J. Bishop,² E. Koshchiy,² E. Aboud,^{1,2,‡} M. Alcorta,³ A. Bosh,^{1,2} K. Hahn,^{4,5} S. Han,⁴ C.E. Parker,² E.C. Pollacco,⁶ B.T. Roeder,² M. Roosa,^{1,2} S. Upadhyayula,^{1,2,§} A.S. Volya,⁷ and G.V. Rogachev^{1,2,8,¶}

¹*Department of Physics and Astronomy, Texas A & M University, College Station, Texas 77843, USA*

²*Cyclotron Institute, Texas A & M University, College Station, Texas 77843, USA*

³*TRIUMF, Vancouver, Canada*

⁴*Ewha Womans University, Seoul, Republic of Korea*

⁵*Center for Exotic Nuclear Studies, Institute for Basic Science, 34126 Daejeon, Republic of Korea*

⁶*IRFU, CEA, Université Paris-Saclay, Gif-Sur-Yvette 91190, France*

⁷*Department of Physics, Florida State University, Tallahassee, Florida 32306, USA*

⁸*Nuclear Solutions Institute, Texas A & M University, College Station, Texas 77843, USA*

(Dated: October 30, 2023)

Background: Spectroscopy of the exotic, neutron unbound beryllium isotope, ^{13}Be , is still a puzzle despite significant experimental efforts.

Purpose: To observe $T=5/2$ states in ^{13}B , establish spin parities and spectroscopic factors, and use isospin symmetry to inform spectroscopy of ^{13}Be .

Methods: Excitation functions for resonance elastic scattering of ^{12}Be on protons was measured in the c.m. energy range from 1 MeV to 5 MeV.

Results: Two $T=5/2$ states in ^{13}B at excitation energies 18.25 MeV and 19.95 MeV were observed. Unambiguous $1/2^+$ and $5/2^+$ spin-parity assignments were made, and spectroscopic factors were established using the R-matrix analysis of the measured $^{12}\text{Be}+p$ excitation functions.

Conclusions: We provide the first direct and unambiguous spin-parity assignments and spectroscopic factors measurements for the resonances in $A=13$ $T=5/2$ isobaric multiplet. This puts us on a solid footing to identify the 2.3 MeV state in ^{13}Be as $5/2^+$ and infer the existence of an s-wave ($1/2^+$) resonance at around 0.6 MeV with relatively small spectroscopic factor.

I. INTRODUCTION

The evolution of nuclear shells with the increasing imbalance between protons and neutrons has been at the forefront of nuclear science for decades. One of the first cases which attracted attention to this phenomenon was a famous parity inversion in ^{11}Be . The ground state of ^{11}Be is $1/2^+$, and not $1/2^-$, as could be expected from simple shell model considerations assuming the “standard” sequence of nuclear shells. The well-established level structure of ^{11}Be below 3 MeV excitation [1] unambiguously indicates that the $2s_{1/2}$ and $1p_{1/2}$ shells are nearly degenerate in this isotope (within a few hundred keV). This degeneracy persists in the heavier beryllium isotope - ^{12}Be . Based on the experimental results and theoretical models, the ground state of ^{12}Be has mixed s^2+p^2 configuration, in which the two valence neutrons occupy the $2s_{1/2}$ and $1p_{1/2}$ shells with nearly equal weights (see also discussion in [2]). It naturally leads to the question of what happens with the addition of one more neutron.

Which shell will be occupied first in ^{13}Be , or more generally, what is the spin-parity of the ground state of ^{13}Be , and what is the level structure of the low-lying excited states in ^{13}Be ? This is the focus of this Letter.

A variety of experimental approaches, summarized in Table I, were used to establish the level structure of this nucleus. Most recent experimental results rely on populating ^{13}Be by neutron or proton removal reaction at high energy, starting from ^{14}Be or ^{14}B , respectively. Yet, due to experimental challenges, the level structure of ^{13}Be remains an open question. This isotope has four more neutrons than the only stable beryllium isotope (^9Be), making it difficult to produce ^{13}Be . It is neutron unbound so that all states in ^{13}Be are broad resonances, and it is possible that four or more states are present in ^{13}Be within the 2 MeV energy range above the neutron decay threshold. These facts lead to significant ambiguities in the analysis of the experimental data.

The results in Table I can be summarized as follows; the most well-established is a state at around 2 MeV above the neutron decay threshold, although its exact excitation energy is uncertain. The spin-parity of this state is believed to be $5/2^+$, but no direct spin-parity assignment was made. Most recent studies seem to agree that the lowest state is an s-wave close to the threshold, with some casting it as a virtual state and others treating it as a resonance. The existence and properties of any states between these two is up for debate. Some experiments suggest a $1/2^-$ state near the ground state, while others suggest there could be another $5/2^+$ state,

* Current affiliation: Facility for Rare Isotope Beams, Michigan State University, East Lansing, MI

† Current affiliation: Center for Exotic Nuclear Studies, Institute for Basic Science, Daejeon, Republic of Korea

‡ Current affiliation: Lawrence Livermore National Laboratory, Livermore, CA

§ Current affiliation: TRIUMF, Vancouver, Canada

¶ rogachev@tamu.edu

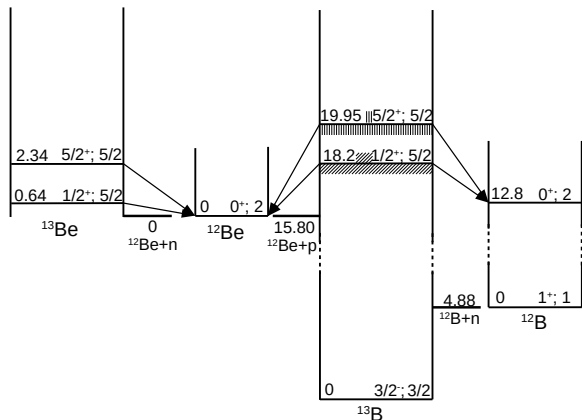


FIG. 1. A partial level structure and decay channels of ^{13}Be and ^{13}B . [10, 11]

and some suggest no additional states. A recent study of ^{13}F [3], the mirror of ^{13}Be , claimed observation of an excited state at 7.06 MeV, which they believe to be the $5/2^+$ excited state, the mirror of the $5/2^+$ in ^{13}Be at around 2 MeV. They were unable to resolve the elusive ground state from the background, however.

There is also significant uncertainty on the theoretical side. Some of the earliest no-core shell model calculations [4] identified the ground state of ^{13}Be to be a $1/2^-$ state at 1.16 MeV above the neutron separation energy, followed by a $5/2^+$, $5/2^-$ and $1/2^+$ level sequence. There were attempts to understand the structure of ^{13}Be using more phenomenological approach, such as the $^{12}\text{Be} + n$ cluster model [5–8], tuning the $^{12}\text{Be}+n$ interaction to the known properties of ^{14}Be . But these models did not result in a definitive conclusion. The ground state in these calculations has been found to be $1/2^+$ in Refs. [5, 7] or $1/2^-$ in Refs. [6, 8]. The application of antisymmetrized molecular dynamics resulted in a low energy $1/2^-$ ground state below a $5/2^+$ excited state [9].

In this Letter, we adopted a different approach to the spectroscopy of ^{13}Be . Instead of populating states in ^{13}Be directly, we study the $T=5/2$ isobaric analog states in ^{13}B and then use isospin symmetry to establish the ^{13}Be level structure. The advantage to this approach is two-fold. First, all $T=5/2$ states in ^{13}B are above the proton decay threshold and can be conveniently populated in $^{12}\text{Be}+p$ resonance elastic scattering, a reaction which has a relatively high cross section (~ 100 mb/sr) and described by well-understood reaction theory. Second, the Coulomb interaction in the $^{12}\text{Be}+p$ partition makes it easier to identify the low-lying s-wave resonance due to the characteristic interference of s-wave with the Coulomb amplitude. The resonance scattering data can be analyzed using the R-matrix approach, allowing unambiguous spin-parity assignments and measurement of the reduced widths (directly related to the spectroscopic factors). Finally, applying a novel active target

TABLE I. Summary of resonances in ^{13}Be suggested in previous experiments.

Reference	E or a MeV or fm	Γ keV	J^π
A.N Ostrowski <i>et al.</i> [12]	2.01 3.12	300 400	$(\frac{5}{2}^+)/(\frac{1}{2}^-)$
A.V. Belozyorov <i>et al.</i> [13]	0.80 2.02 2.90 4.94 5.89 7.8		$(\frac{1}{2}^-)$
M. Thoennessen <i>et al.</i> [14]	< -10 fm		$(\frac{1}{2}^+)$
H. Simon <i>et al.</i> [15]	-3.2 fm		$(\frac{1}{2}^+)$
Y. Kondo <i>et al.</i> [16]	-3.4 fm		$(\frac{1}{2}^+)$
	0.51	450	$(\frac{1}{2}^-)$
	2.39	2400	$(\frac{5}{2}^+)$
Y. Aksyutina <i>et al.</i> [17]	0.81 0.46/0.44 2.07/1.95 2.98/3.02	2.1 0.11/0.39	
G. Randisi <i>et al.</i> [18]	0.40 0.85 2.35	800 300 1500	$(\frac{1}{2}^+)$ $(\frac{3}{2}^+)$ $(\frac{5}{2}^+)$
B.R. Marks <i>et al.</i> [19]	0.40 1.05 2.56	800 500 2560	$(\frac{1}{2}^+)$ $(\frac{3}{2}^+)$ $(\frac{5}{2}^+)$
G. Ribeiro <i>et al.</i> [20]	0.86 2.11	1.70	$(\frac{1}{2}^+)$ $(\frac{5}{2}^+)$
A. Corsi <i>et al.</i> [21]	0.48 2.3 5.1 5.7		$(\frac{1}{2}^+)$ $(\frac{1}{2}^-)$ $(\frac{3}{2}^+)$ $(\frac{5}{2}^+)$

experimental technique allowed us to accumulate sufficient statistics despite the low intensity of exotic ^{12}Be beam between 400 and 1,000 pps (it varied during the run).

II. EXPERIMENT

The excitation function for $^{12}\text{Be} + p$ resonance elastic scattering was measured at TRIUMF (British Columbia, Canada) using the ISAC-II facility [22]. ^{12}Be ions were produced from a tantalum target and accelerated through the ion transport system to the SC-linac. The SC-linac accelerated the ^{12}Be ions to 6 MeV/u. This energy allowed the measurement of the excitation function in the center of mass frame starting from 5.5 MeV down to about 1 MeV. This corresponds to the excitation energy region in ^{13}B where low-lying $T=5/2$ isobaric analogue states are expected (see Figure 1).

Measurements were performed using the Texas Active Target (TexAT) detector, shown in Figure 2 [23]. As a Time Projection Chamber (TPC), TexAT uses a

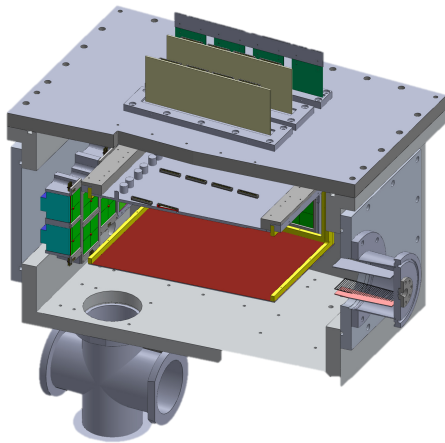


FIG. 2. A cutaway view of TexAT showing the Micromegas plate, Si/CsI detector wall at the back and ionization chamber.

highly-segmented Micro-Mesh Gaseous Structure (Micromegas) detector to record tracks of charged particles. For additional gas gain, a Gas Electron Multiplier (GEM) is placed before the Micromegas mesh. Tracks of the beam particle and the heavy and light recoil particles are recorded by the TPC. As an active target TPC, TexAT uses the same gas as a target and an active medium of the detector. In TexAT, an array of silicon detectors are placed at the forward wall of the chamber backed by CsI crystal scintillators to measure the energy of the light recoil particles. The particle tracks in the detector are used to reconstruct the reaction kinematics in conjunction with the total energy measurements in the silicon and CsI detectors. The signal from the GEM detector was used to count beam ions.

The TexAT was filled with 260 Torr of isobutane gas. At this pressure, the ^{12}Be beam ions stop before the last 1/8 of the active region of the TPC. The TexAT micromegas were divided into two gain regions, a low gain region for the beam and heavy recoil and a high gain region sensitive to protons by applying a different bias to the Micromegas pads. The low gain region was the first 7/8 of the highly segmented central region. The high gain region was the side regions and the last 1/8 of the segmented central region. General Electronics for TPCs (GET) [24], combined with the GANIL DAQ [25] were used for the readout. More details on the TexAT active target detector can be found in [23].

The triggers were produced by any charged particle hitting the silicon detectors and depositing energy above the threshold set in GET electronics (generally around 1 MeV). Since ^{12}Be ions are stopped in the gas volume about 10 cm before the forward silicon detector wall, the majority of recorded events were due to electrons from β -decay of ^{12}Be hitting the Si detectors, with the total event rate of about 50 Hz. However, such events are easy to identify as they produce no tracks in the TPC.

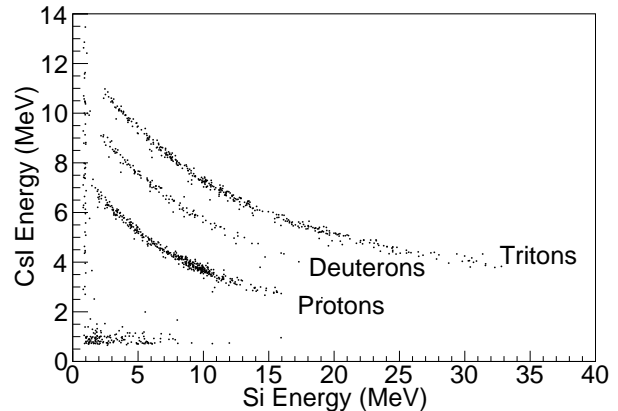


FIG. 3. The energy deposited in the Si detectors vs the CsI detectors for the 620- μm -thick Si detectors. Protons, deuterons, and tritons can be clearly seen as labeled.

III. ANALYSIS

The complete kinematics of the reactions measured in this experiment can be determined from the tracks in the TPC and the energies measured in the Si-CsI arrays. The dE-E curves for the events that punched through the Si detectors are plotted in Figure 3, which shows a clear separation between protons, deuterons, and tritons. In the TPC, two pieces of information can be utilized with the Si-CsI array energy: the vertex position where the reaction occurred and the endpoint of the heavy recoil track (which always stops in the TPC). The energy vs endpoint plot (Fig. 4) shows bands for the reactions present. The dominant reactions are the $^{12}\text{Be}(p,p)^{12}\text{Be}$, $^{12}\text{Be}(p,t)^{10}\text{Be}$, and $^{12}\text{Be}(p,d)^{11}\text{Be}$ reactions with lighter bands for the (p,p') and (p,t) populating low-lying states in ^{12}Be and ^{10}Be respectively.

Using Figures 3 and 4, the (p,p) elastic scattering, (p,d) , and (p,t) reactions can be identified at energies above the proton punch-through in the Si detectors (≈ 8 MeV for most of the Si detectors used in this experiment). This is done by gating on the p/d/t banana in the Si-CsI ΔE -E 2D scatter plot (Fig. 3) and selecting the proper kinematic region in the total energy of the light recoil vs heavy recoil endpoint (Fig. 4) plots. In the energy region below the Si punch-through, the (p,p) and (p,d) reactions are more difficult to separate. This is because our gas gain in TPC was relatively low and did not allow for unambiguous discrimination of protons from deuterons using energy losses in the gas and also due to the fact that (p,p) and (p,d) reaction kinematics is too similar in the energy and angular range of interest for these measurements. As a result, in spite of having complete kinematics measurement, we had to subtract the (p,d) background in the energy range below 8 MeV (this corresponds to about 3 MeV in c.m. for the $p+^{12}\text{Be}$ excitation function). To do that, we extrapolated the measured yield of deuterons from the $^{12}\text{Be}(p,d)$

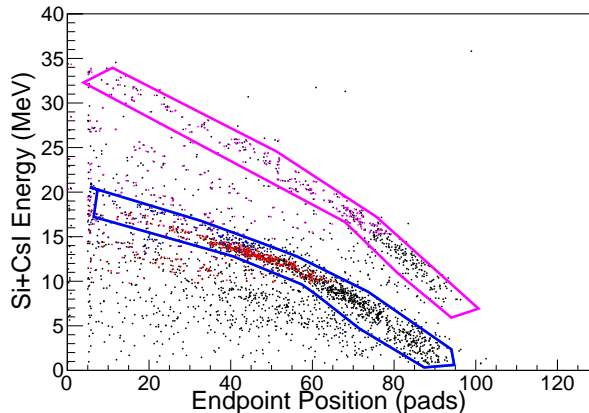


FIG. 4. Plot of the location in the TPC where the heavy recoil track ends vs the energy in the Si+CsI telescopes for the most-central detectors. The red points are protons, the blue are deuterons, and the magenta are tritons as identified by the Si vs CsI plot. The blue and magenta graphical cuts correspond to the kinematics of the (p,p) elastic scattering and the $^{12}\text{Be}(p,t)^{10}\text{Be}(\text{g.s.})$ reaction, respectively.

reaction within the proton graphical cut at higher energies to lower energies using a smooth phenomenological function that assumes nearly energy-independent cross-section in the relevant energy range from 1.5 to 3 MeV in c.m. and describes the experimental deuteron yield from 3 to 5 MeV in c.m.

The $^{12}\text{Be}(p,p)^{12}\text{Be}(\text{g.s.})$ excitation functions are shown in Figure 5. The experimental energy resolution of the $p+^{12}\text{Be}$ excitation functions is within the energy bin in Figure 5 for all c.m. energies. The data was grouped based on the segmentation of the silicon detectors in TexAT. Six of the silicon detectors were used for the excitation function, grouped based on symmetry. The top left excitation function is for the central detector, top right is the exposed bottom half of the detector above the central detector, bottom left is the inner columns of the four detectors next to the central pair, and the bottom right being the outer columns of the four detectors next to the central pair. The angles are defined by the vertex position corresponding to the energy bin and the centroid of the detector regions.

IV. RESULTS AND DISCUSSION

Elastic scattering of protons on ^{12}Be can populate both the $T=3/2$ and $T=5/2$ resonances at excitation energies above the proton decay threshold (15.80 MeV). $T=3/2$ resonances have many open decay channels, such as neutron emission to the $T=1$ states in ^{12}B , since the neutron decay threshold is only 4.88 MeV (see Fig. 1). Conversely, the $T=5/2$ resonances have few isospin-conserving decays. Only proton decay to the $^{12}\text{Be}(\text{g.s.})$ is possible up to 17.61 MeV ^{13}B excitation, at which en-

ergy the isospin-conserving neutron decay to the $T=2$ 0^+ state at 12.8 MeV in ^{12}B (the isobaric analog of the $^{12}\text{Be}(\text{g.s.})$) opens. As a result, it is natural to expect that the $T=5/2$ states with significant single-particle spectroscopic factors (if there are any) will dominate the $p+^{12}\text{Be}$ elastic scattering excitation function. The validity of this assumption was confirmed recently for a different nucleus - ^9Be . It was demonstrated in Ref. [26] that the excitation function for the $p+^8\text{Li}$ resonance elastic scattering is dominated by the T -high ($T=3/2$) states in the energy region where strong $T=3/2$ states are present.

Two single-particle states can be expected in the spectrum of ^{13}Be from simple shell model considerations. Assuming the closed $p1/2$ shell in ^{12}Be ($N=8$), the $5/2^+$ ($1d5/2$) and $1/2^+$ ($2s1/2$) states are naturally expected to be the lowest single-particle configurations in ^{13}Be . Indeed, a shell model calculation using the FSU interaction [27] restricted to no cross-shell excitations ($0\hbar\omega$ space) produces two strong single-particle states, the $1/2^+$ at 179 keV excitation ($S=0.91$) and $5/2^+$ at 2.045 MeV ($S=0.69$). However, it is clear that cross-shell excitations must be considered. The ground state $1/2^-$ comes from $1\hbar\omega$, and another $5/2^+$ of $2\hbar\omega$ configuration appears at a lower excitation energy of 1.782 MeV which is clearly mixed with the $5/2^+$ mentioned previously. Similar mixing occurs in the ground state of ^{12}Be making the spectroscopic factors sensitive to configuration mixing. We will discuss this mixing later, nevertheless, a good starting point for the analysis of the measured $^{12}\text{Be}+p$ excitation function is to see if it can be reproduced with just two $T=5/2$ states, the $1/2^+$ and $5/2^+$ expected within simplified $0\hbar\omega$ model space.

The R-Matrix analysis performed with the code MinRMMatrix [28] indicates that a good fit can be achieved by including a $1/2^+$ resonance with c.m. energy $E = 2.45(1)$ MeV and a $5/2^+$ resonance with c.m. energy $E = 4.15(6)$ MeV (Figure 5). This fit has four free parameters, the c.m. energies, and the spectroscopic factors for the two states. Only two channels were used in the fit - the isospin-allowed proton and neutron decays. The reduced widths for each $T=5/2$ state were calculated from Equations 1-2, where S is a spectroscopic factor and C^2 are squared isospin Clebsch-Gordan coefficients for the $p+^{12}\text{Be}$ and $n+^{12}\text{B}(T=2)$ channels. All four excitation functions were fit with the same parameters simultaneously. The parameters for the observed $T=5/2$ states are shown in Table II.

$$\gamma_{p+^{12}\text{Be}(T=2)}^2 = S(C_{\frac{1}{2}^+}^{\frac{5}{2}^+})^2 \gamma_{sp}^2 = \frac{1}{5} S \gamma_{sp}^2 \quad (1)$$

$$\gamma_{n+^{12}\text{B}(T=2)}^2 = S(C_{\frac{1}{2}^-}^{\frac{5}{2}^+})^2 \gamma_{sp}^2 = \frac{4}{5} S \gamma_{sp}^2 \quad (2)$$

The experimental result is consistent with the observation of two $T=5/2$ states with spin-parities $1/2^+$ and $5/2^+$. There is no need for any additional $T=5/2$ states or $T=3/2$ background. Using the isospin symmetry and the fact that the wavefunction of the $T=5/2$ state in ^{13}B

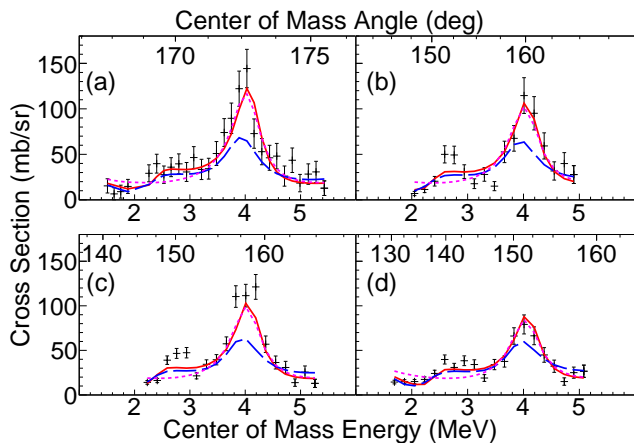


FIG. 5. The excitation function for $^{12}\text{Be}+p$ resonance elastic scattering. The solid red curve in an R-matrix fit with $1/2^+$ and $5/2^+$ states. The R-matrix calculation with a $1/2^-$ state instead of a $1/2^+$ state is shown in magenta dots, and a $3/2^+$ excited state instead of $5/2^+$ is shown in blue dashes.

TABLE II. Best fit R -matrix parameters for the $T=5/2$ states in ^{13}B with a channel radius of 4.2 fm and $\gamma_{sp}^2=2.55$ MeV. E_{ex} is the excitation energy in ^{13}B , E_{cm} is the center of mass energy, Γ is the total width, and S is the spectroscopic factor.

J^π	E_{ex} MeV	E_{cm} MeV	Γ keV	S
1^+	18.25 ± 0.1	2.45 ± 0.1	660^{+400}_{-250}	$0.16^{+0.09}_{-0.06}$
$5/2^+$	19.95 ± 0.06	4.15 ± 0.06	600 ± 100	0.49 ± 0.08

is dominated by the $n+^{12}\text{B}(T=2)$ configuration, we evaluate the c.m. energies of the respective $1/2^+$ and $5/2^+$ states in ^{13}Be by subtracting the threshold for neutron decay to the first $T=2$ state in ^{12}B from the ^{13}B excitation energy. This results in $1/2^+$ and $5/2^+$ resonances in ^{13}Be unbound with respect to the neutron decay by 0.6(1) MeV and 2.34(6) MeV, respectively. The energy of the $5/2^+$ resonance is in nearly perfect agreement with Refs. [16, 18, 19]. The $1/2^+$ resonance energy is also in good agreement with Ref. [19].

The spectroscopic factor of the observed $T=5/2$ $1/2^+$ state is small (≈ 0.2). The reduction from $S=0.91$ highlights the importance of mixing. Apart from mixing in ^{13}Be , the s^2 and p^2 configurations are believed to be nearly degenerate in ^{12}Be . It is also confirmed by the shell model analysis using FSU interaction. Therefore, it is essential to include all mixing and, in particular, the mixing of the $0\hbar\omega$ and $2\hbar\omega$ configurations in the ^{12}Be . Such mixing leads to very different shell model predictions for the ^{13}Be states, which is shown in Table III. In this model, the $1/2^+$ spectroscopic factor is much reduced and agrees with the experimental value within the uncertainty. For the $5/2^+$ state, both the spectroscopic factor and the excitation energy with respect to the $1/2^+$ are reproduced (within 2σ).

The shell model calculations with the FSU interaction

TABLE III. Level structure of ^{13}Be predicted by the shell model with FSU Hamiltonian, which includes mixing of configurations in ^{12}Be and ^{13}Be

J^π	E_{ex}	S
$1/2^+$	0.00	0.23
$1/2^-$	0.03	0.49
$3/2^-$	0.97	0.68
$5/2^+$	1.43	0.69
$3/2^-$	1.90	0.12
$5/2^+$	2.21	0.01

predict two negative parity states below the first $5/2^+$. The possibility of a negative parity ground state has been suggested in other theoretical studies [6, 8] and experimentally [14]. We now need to explore if negative parity state(s) is(are) consistent with the experimental data presented in this study.

Replacing the $1/2^+$ ground state with a $1/2^-$ ground state leads to a significant change in the shape and magnitude of the cross section at c.m. energies below 3 MeV, underestimating the experimental cross sections (see Figure 5). Most importantly, without the $1/2^+$ resonance, there is no characteristic decrease of the cross section near 2 MeV that is caused by destructive interference between the Coulomb amplitude and the s-wave resonance. We conclude that the $1/2^+$ resonance is essential to reproduce the experimental data.

The peak at 4 MeV is described well by a $5/2^+$ resonance. The $3/2^+$ spin-parity assignment for this resonance is not consistent with the data because it leads to the significantly lower cross section near 4 MeV, as shown by the blue dashed curve in Figure 5.

We tried to add the $1/2^-$ and the $3/2^-$ states simultaneously and one by one, keeping the $1/2^+$ and the $5/2^+$ states in the fit. It turned out that the sensitivity of our experimental data to the negative parity states is low. Each of the tried configurations can describe the measured excitation function because the negative parity states make relatively small contributions. Properties of the positive parity states remain the same within the experimental uncertainties regardless if the negative parity states are present or not.

V. CONCLUSION

The structure of low-lying states in ^{13}Be is a topic of great interest and much debate. Experimental and theoretical studies have thus far been unable to make definitive conclusions about the structure of this nucleus. This nucleus is unbound and likely has several broad overlapping resonances in the low-energy region, making it difficult to interpret the experimental results. We took advantage of the isospin symmetry to study the spectroscopy of the $T=5/2$ isobaric analogues in ^{13}B , populating them using $p+^{12}\text{Be}$ resonance scattering reaction. The R-matrix analysis of the excitation functions for the

$p+^{12}\text{Be}$ resonance elastic scattering, measured by the active target detector TexAT in the c.m. energy range from 1 to 5 MeV, allowed us to unambiguously identify two $T=5/2$ resonances at 18.25 and 19.95 MeV excitation energies in ^{13}B and provide unique spin-parity assignments, $1/2^+$ and $5/2^+$, respectively. To explain the relatively small experimental spectroscopic factor of the $1/2^+$ state in the framework of the shell model, one needs to include strong s^2 / p^2 configuration mixing for the ^{12}Be states, providing another piece of evidence for the near-degeneracy of the s - and p - shells in this nucleus.

We cannot provide a definitive answer to the question of the spin-parity of the ^{13}Be ground state. A good fit to the measured $p+^{12}\text{Be}$ excitation function can be achieved with only the $1/2^+$ and $5/2^+$ $T=5/2$ states. No negative parity states are required. Yet, one can include the negative parity states ($1/2^-$ and $3/2^-$) and still obtain a good fit, because the $1/2^+$ and the $5/2^+$ states define the main features of the excitation functions. An intriguing opportunity to resolve this problem would be to measure the

neutron decay of the $T=5/2$ states in ^{13}B to the first $T=2$ state in ^{12}B at 12.8 MeV. If the ground state in the $T=5/2$ $A=13$ spectrum has negative parity, it would be a relatively narrow resonance (few hundred keV) which should be clearly visible in the spectrum of neutrons from the $^{12}\text{Be}(p,n)^{12}\text{B}(0^+, T=2)$ reaction.

VI. ACKNOWLEDGMENTS

The authors are grateful to the TRIUMF accelerator team, which provided high-quality secondary ^{12}Be beam, and to Dr. V.Z. Goldberg for valuable comments and discussion. This work was supported by the U.S. Department of Energy, Office of Science, Office of Nuclear Science under awards no. DE-FG02-93ER40773 and DE-SC0009883, and by National Nuclear Security Administration through the Center for Excellence in Nuclear Training and University-Based Research (CENTAUR) under grant number DE-NA0003841.

-
- [1] J. H. Kelley, E. Kwan, J. E. Purcell, C. G. Sheu, and H. R. Weller, *Nucl. Phys. A* **880**, 88 (2012).
 - [2] R. Sherr and H. T. Fortune, *Phys. Rev. C* **60**, 064323 (1999).
 - [3] R. J. Charity, T. B. Webb, J. M. Elson, D. E. M. Hoff, C. D. Pruitt, L. G. Sobotka, K. W. Brown, G. Cerizza, J. Estee, W. G. Lynch, *et al.*, *Phys. Rev. Lett.* **126**, 132501 (2021).
 - [4] N. Poppelier, L. Wood, and P. Glaudemans, *Phys. Lett. B* **157**, 120 (1985).
 - [5] P. Descouvemont, *Phys. Rev. C* **52**, 704 (1995).
 - [6] M. Labiche, F. M. Marqués, O. Sorlin, and N. Vinh Mau, *Phys. Rev. C* **60**, 027303 (1999).
 - [7] T. Tarutina, I. Thompson, and J. Tostevin, *Nucl. Phys. A* **733**, 53 (2004).
 - [8] G. Blanchon, N. V. Mau, A. Bonaccorso, M. Dupuis, and N. Pillet, *Phys. Rev. C* **82**, 034313 (2010).
 - [9] Y. Kanada-En'yo, *Phys. Rev. C* **85**, 044320 (2012).
 - [10] J. H. Kelley, J. E. Purcell, and C. Sheu, *Nucl. Phys. A* **968**, 71 (2017).
 - [11] F. Ajzenberg-Selove, *Nucl. Phys. A* **523**, 1 (1991).
 - [12] A. N. Ostrowski *et al.*, *Z. Phys. A* **343**, 489 (1992).
 - [13] A. V. Belozorov, R. Kalpakchieva, Y. E. Penionzhkevich, Z. Dlouhý, S. Piskor, J. Vincour, H. G. Bohlen, M. von Lucke-Petsch, A. N. Ostrowski, D. V. Alexandrov, *et al.*, *Nucl. Phys. A* **636**, 419 (1998).
 - [14] M. Thoennessen, S. Yokoyama, and P. G. Hansen, *Phys. Rev. C* **63**, 014308 (2000).
 - [15] H. Simon, M. Meister, T. Aumann, M. J. G. Borge, L. V. Chulkov, U. Datta Pramanik, T. W. Elze, H. Emling, C. Forssén, H. Geissel, *et al.*, *Nucl. Phys. A* **791**, 267 (2007).
 - [16] Y. Kondo, T. Nakamura, Y. Satou, T. Matsumoto, N. Aoi, N. Endo, N. Fukuda, T. Gomi, Y. Hashimoto, M. Ishihara, *et al.*, *Phys. Lett. B* **690**, 245 (2010).
 - [17] Y. Aksyutina, T. Aumann, K. Boretzky, M. J. G. Borge, C. Caesar, A. Chatillon, L. V. Chulkov, D. Cortina-Gil, U. Datta Pramanik, H. Emling, *et al.*, *Phys. Rev. C* **87**, 064316 (2013).
 - [18] G. Randisi, A. Leprince, H. Al Falou, N. A. Orr, F. M. Marqués, N. L. Achouri, J.-C. Angélique, N. Ashwood, B. Bastin, T. Bloxham, *et al.*, *Phys. Rev. C* **89**, 034320 (2014).
 - [19] B. R. Marks, P. A. DeYoung, J. K. Smith, T. Baumann, J. Brown, N. Frank, J. Hinnefeld, M. Hoffman, M. D. Jones, Z. Kohley, *et al.*, *Phys. Rev. C* **92**, 054320 (2015).
 - [20] G. Ribeiro, E. Nácher, O. Tengblad, P. Díaz Fernández, Y. Aksyutina, H. Alvarez-Pol, L. Atar, T. Aumann, V. Avdeichikov, S. Beceiro-Novo, *et al.* (R^3B Collaboration), *Phys. Rev. C* **98**, 024603 (2018).
 - [21] A. Corsi, Y. Kubota, J. Casal, M. Gómez-Ramos, A. Moro, G. Authelet, H. Baba, C. Caesar, D. Calvet, A. Delbart, *et al.*, *Phys. Lett. B* **797**, 134843 (2019).
 - [22] E. L. R and M. M, The ISAC post-accelerator, *Hyperfine Interactions* **225**, 79 (2014).
 - [23] E. Koshchiy, G. Rogachev, E. Pollacco, S. Ahn, E. Uberseder, J. Hooker, J. Bishop, E. Aboud, M. Barbui, V. Goldberg, *et al.*, *Nucl. Inst. Meth. Phys. Res. A* **957**, 163398 (2020).
 - [24] E. Pollacco, G. Grinyer, F. Abu-Nimeh, T. Ahn, S. Anvar, A. Arokiaraj, Y. Ayyad, H. Baba, M. Babo, P. Baron, *et al.*, *Nucl. Inst. Meth. Phys. Res. A* **887**, 81 (2018).
 - [25] X. Grave, R. Canedo, J.-F. Clavelin, S. Du, and E. Legay, in *14th IEEE-NPSS Real Time Conference, 2005*. (2005) pp. 5 pp.-.
 - [26] C. Hunt, G. V. Rogachev, S. Almaraz-Calderon, A. Aprahamian, M. Avila, L. T. Baby, B. Bucher, V. Z. Goldberg, E. D. Johnson, *et al.*, *Phys. Rev. C* **102**, 014615 (2020).
 - [27] R. S. Lubna, Ph.D. thesis, Florida State University (2019).
 - [28] E. D. Johnson, Ph.D. thesis, Florida State University (2008).